RSC Advances

ROYAL SOCIETY OF CHEMISTRY

www.rsc.org/advances

Cite this: DOI: 10.1039/c0xx00000x

www.rsc.org/xxxxxx

ARTICLE TYPE

Electrochemical Supercapacitor Development Based on Electrodeposited Nickel Oxide Film

S.T. Navale[a], V.V. Mali[a], S.A. Pawar[a], R.S. Mane[b, c], M. Naushad[c], F. J. Stadler[d], and V.B. Patil[a,*]

A nickel oxide (NiO) electrode has been synthesized electrochemically, which is envisaged for supercapacitor application. The structural, morphological, and phase-purity confirmation studies of NiO films were undertaken using X-ray diffraction, Fourier transforms infrared spectroscopy (FTIR), field-emission scanning electron microscopy, and contact angle measurements. Films of NiO were amorphous in phase, as there was no any reflecting plane in the X-ray diffraction pattern. The presence of characteristic bands in FTIR and X-ray photoelectron spectroscopy analysis corroborated for NiO structure. The NiO film surface was smooth with very fine elongated particles (~70 nm) and hydrophilic in character (57°). The supercapacitive performance of NiO electrode tested using cyclic voltammetry measurement in 0.5M Na_2SO_4 electrolyte within potential range of −1.2 - +1.2 V demonstrated to have a specific capacitance as high as 458 Fg^{-1} at 5mV/s. The obtained specific energy, specific power and Coulomb efficiency of NiO electrode were 10.90 Wh kg^{-1}, 0.89 kW kg^{-1}, and 98%, respectively.

1. Introduction

In recent years, electrochemical capacitors or supercapacitors have attracted considerable attention because of their high-power delivery within a very short time and long cycle life, which can store energy used for hybrid electric vehicles and mobile electronic devices [1, 2]. Generally, supercapacitors are classified into two types; (i) electric double-layer capacitors, which are carbon-based materials with a high surface area, and (ii) faradic pseudo-capacitors, which are made of metal oxides.Various transition-metal oxides such as SnO_2, RuO_2, Co_3O_4, Fe_2O_3, MnO_2, etc., are being studied for supercapacitor applications. Among these, amorphous hydrous RuO_2 is the most promising materials envisaged for supercapacitors application because of its high specific capacitance (SC), excellent reversibility, and long cycle life. However, RuO_2 is expensive, toxic, and scarce in nature, which limits its practical application. Accordingly, there is a strong incentive to find alternative electrode materials, which would be inexpensive and exhibit pseudocapacitance behavior similar to that of amorphous $RuO_2 \cdot xH_2O$. To this end, much attention is now being focused on the oxides of manganese [3], nickel [4], cobalt [5], vanadium [6] and copper [7], etc., as candidates for electrode materials. As an alternative, we propose low-cost material nickel oxide (NiO) for use as supercapacitor. Thin films of NiO have been prepared previously by various methods such as sol–gel [8], chemical vapor deposition [9], electrodeposition [10], and spray pyrolysis [11]. Chemical methods are being regularly applied for the synthesis of metal oxide/chalcogenide materials in thin films rather than physical methods, since they have good control on growth process. Chemical methods have their own advantages such as simplicity, reproducibility, non-hazardousness, cost-effectiveness, etc.

[a]*Functional Materials Research Laboratory (FMRL), School of Physical Sciences, Solapur University, Solapur-413 255, M.S., India. Tel: +912172744770 (Ext-202), E-mail: drvbpatil@gmail.com,*[b]*School of Physical Sciences, Swami Ramanand Teerth Marathwada University Nanded-431606, India*
[c]*Advanced Materials Research Chair, Department of Chemistry, College of Science, Bld#5, King Saud University, Riyadh, Saudi Arabia,* [d]*Shenzhen University, Nanshan District Key Lab for Biopolymers and Safety Evaluation,College of Materials Science and Engineering, Shenzhen, Guangdong, China.*

Among different chemical methods electrodeposition (ED) is economical and easy to operate and the product quality is uniform and competitive with physical methods. There are three different ways (i.e. varying electric field, constant voltage and constant current), by which one can apply the electric field in ED process. These three different types of applied electric fields significantly have an impact on the surface morphology, crystal structure and, hence, the supercapacitive properties of deposited materials.

In the present investigation, we report electrochemical supercapacitor application of NiO deposited onto stainless-steel (SS) substrate using ED process. The structural and surface morphological studied were undertaken using by X-ray diffraction (XRD), Fourier transform infrared spectroscopy (FTIR), X-ray photoelectron spectroscopy (XPS) and field-emission scanning electron microscopy (FESEM) measurements, respectively. The capacitive properties were investigated with the using cyclic voltammetry, electrochemical impedance spectroscopy, i.e., Nyquist and galvanostic charge–discharge plots.

2. Experimental details

2.1 Synthesis of NiO thin film electrode

The NiO thin film electrode was synthesized onto SS substrate (grade 304, 0.2mm thickness) from AR grade Ni. $(CH_3COOCH)_2 \cdot 4H_2O$ as a source of Ni, using ED process. Prior to deposition, the substrate was polished with emery paper to a rough finish, washed to remove the emery particles and then air-dried. The electrochemical synthesis of NiO was performed in a conventional three-electrode electrochemical cell, containing SS substrate as a working electrode, graphite plate of 2 cm^2 surface area as a counter electrode and saturated calomel electrode (SCE) as a reference electrode (shown in Figure 1). The deposition of well adherent and uniform gray product, indicating the presence of $Ni(OH)_2$, film electrode was obtained from 0.1M nickel acetate solution at room temperature (300 K) by applying a constant potential of +1.8 V/SCE for the deposition time of 50 min. The $Ni(OH)_2$ electrode annealed at 400 °C in air atmosphere for 30 min in tubular furnace for the formation of the NiO. Mass of deposited product was estimated from the gravimetric weight difference method by using sensitive microbalance and $t = \Delta m / (\rho \times A)$ relation. Here, 'Δm' is the mass of the film deposited on the substrate, 't' is the thickness of deposited electrode, 'A' the area of the deposited film and 'ρ' the density of the deposited

material i.e. NiO which is 6.67 g/cm^3 in the bulk form. The optimum thickness obtained for NiO thin film was 0.602 µm for 50 min, beyond which with increase in time film thickness i.e. deposited mass degraded, as it was peeling off from the substrate.

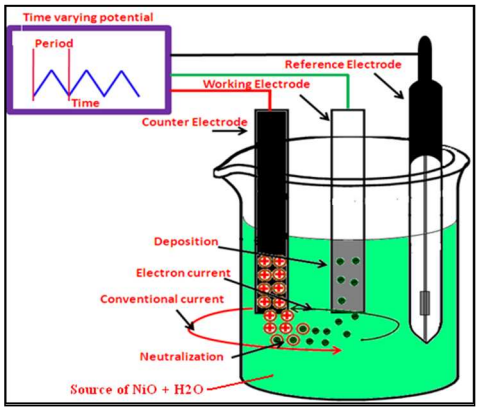

Figure 1:.Schematic of formation of $Ni(OH)_2$ electrode.

2.2 Material characterizations

The XRD pattern was carried out using X-ray diffractometer (Model: PW-3710, Holland) using CuKα radiation (λ = 1.5406 Å) in 2θ range of 10–80° and for XPS measurement, VG, Multilab 2000, Thermo VG, Scientific, UK, unit was preferred. FTIR measurement was recorded between 4000 and 500 cm^{-1} at a spectral resolution of 2 cm^{-1} on a PerkinElmer 100 spectrophotometer in presence of KBr pellets at room temperature. Surface morphology was confirmed from the FESEM (MIRA3 TESCAN operating at 20 kV) digital photoimage. The electrochemical supercapacitor performance of the NiO electrode was tested with the help of cyclic voltammetry (C-V) plots.

3. Results and discussion

3.1 NiO thin film formation mechanism

A cathodic electrodeposition process has been used in forming films of different oxides [12–14]. It was pointed out that the electrodeposition method is similar to that of the wet chemical method, as in both cases the use of electrogenerated base instead of alkali is unavoidable [14]. Deposition of $Ni(OH)_2$ film onto the SS substrate by electrodeposition was carried out under above-mentioned conditions. Formation of $Ni(OH)_2$ in alkaline medium takes place through;

$$Ni(CH_3COOCH)_2.4H_2O + H_2O \rightarrow Ni(OH)_2 \quad \ldots(1)$$

This after annealing develops NiO as;

$$Ni(OH)_2 \rightarrow NiO \quad \ldots(2)$$

The mechanism shows that, in an alkaline bath formation of $Ni(OH)_2$ dominates initially which then is converting to NiO. NiO films with different thicknesses were obtained by varying the deposition time period. The film thickness was increased with increase in the deposition time. The accurate measurement of film thickness was not possible because of the porosity of the NiO deposited; therefore, the as-deposited weight (g cm^{-2}) of NiO film on SS substrate was measured [15]. Maximum thickness (0.602 µm) was obtained for the time period of 50 min. For further deposition period, the deposited weight declined, which could be due to the fall-off of porous deposit similar to electrodeposited RuO_2 films [16].

3.2 Structural elucidation studies

Figure 2(a) shows the XRD patterns of stainless steel (SS) and NiO thin film on SS. No clearly identifiable diffraction peak other than SS substrate was observed in XRD pattern, which could be due to dominance of amorphous colloidal NiO particles. The peaks obtained due to SS were indexed by the symbol SS. We believe amorphous NiO would be beneficial for supercapacitor application, which generally permits an easier access of its atoms for redox reactions [17].

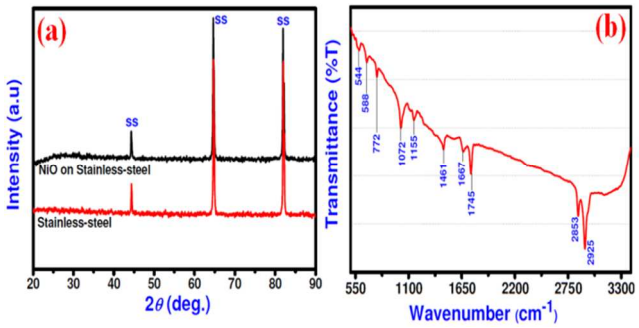

Figure 2: (a) XRD pattern of SS and NiO thin film on SS and (b) FTIR spectrum of NiO.

3.3 FTIR studies

Various chemical bondings present in NiO were confirmed by FTIR analysis [10]. Figure 2(b) shows the FTIR spectrum of NiO. The FTIR spectrum of NiO reveals the vibrations at 1072 cm^{-1}, 1155 cm^{-1}, 1461 cm^{-1}, 1667 cm^{-1} and 1745 cm^{-1} supporting for the presence of –OH groups and vibrations at 2853 cm^{-1} and 2925 cm^{-1} are for H_2O. The bands in the region 772–500 cm^{-1} provide information about NiO. The peaks at 544 cm^{-1}, 588 cm^{-1} and 772 cm^{-1} correspond to the metal–oxygen (Ni–O) vibrational modes of the spinel compound; also these three peaks are the characteristics of spinel structure [11]. The presence of Ni–O bonds, and –OH groups evidenced the formation of NiO.

3.4 Surface morphological studies

Figure 3(a) shows an FESEM image of NiO thin film. The adherence of the films to the substrates was so good that the films were not peeled or also scraped off with SS knives. The NiO film surface was found to be smooth and composed of very fine elongated particles connected by spherical lobes. Also from the FESEM image, overgrowth of clusters is clearly seen. Initially as-grown crystallites could increase their sizes and might come close to each other as deposition proceeds.

The NiO film surface was well covered without any pinholes and cracks which may be able to provide higher surface area for electrochemical redox reaction when used in electrochemical supercapacitors.TEM image of NiO thin film is shown in Figure 3(b). Image clearly shows that very fine elongated particles with average diameter ~70 nm are interconnected each other; indicating synthesized NiO is in nanometer range.

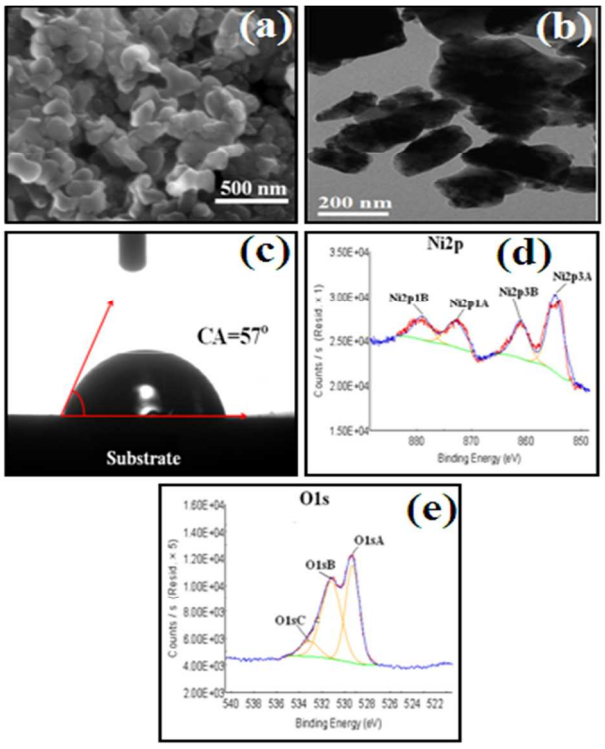

Figure 3: (a) FESEM image, (b) TEM image, (c) water contact angle measurement, (d)Ni 2p core level spectrum of NiO and (e) O 1s XPS spectra of NiO film.

3.6 Surface wettability test

The NiO film annealed at 400 °C was used in surface wettability test (water contact angle measurement). The wetting of solid with water, where air is the surrounding medium, is dependent on the relation between the interfacial tensions (water/air, water/ solid and solid/air). The ratio between these tensions determines the contact angle 'θ' between water droplets on a given surface. A contact angle of 0° means complete wetting, and a contact angle of 180° corresponds to complete non-wetting. Both super-hydrophilic and super-hydrophobic surfaces are important for practical applications. The average contact angle was obtained by measuring for at least five separate drops on each NiO film surface by delivering de-ionized water with a microsyringe. Measurement of surface water contact angle is inversely proportional to the wettability and can be determined by Young's relation. Figure 3(c) shows the water contact measurement for nickel oxide thin film. From Figure 3 (c), it is observed that the NiO thin film is hydrophilic as the water contact angle is 57° (less than 90°). This may be due to the strong cohesive force between the water droplet and oxide of the NiO. This specific character finds usefulness while making intimate contact of aqueous electrolyte with electrode surface in supercapacitor application. Hydrophilic nature of NiO tentatively demonstrated for the feasibility of NiO film surface in electrochemical supercapacitive performance as it is known that in the electrochemical capacitors, hydrophilic surface of the electrode is an essential factor for enhancing redox reaction activity [18].

3.4 XPS analysis

XPS is an effective tool to show surface composition followed surface states existing in the synthesized thin film/powder product. The formation of NiO was also confirmed from the XPS survey spectrum. Figures 3(d) &(e) present the core level Ni 2p and O 1s XPS spectra of NiO, respectively. The core level spectrum of Ni 2p [Fig. 3(d)] has confirmed four peaks namely Ni2p1A, Ni2p1B, Ni2p3A and Ni2p3Blocated at binding energies of 872.86, 878.94, 854.66, and 861.01eV, respectively, with an energy difference of 18.2 eV, and 17.93 eV; which is main characteristic of Ni^{2+} state [19].The O 1s core level spectrum of NiO is shown in Figure 3(e). The main binding energy peak is at 529.03 eV, which corresponds to O^{2-} in the nickel oxide [20]. While, the peaks with binding energies at 531.18 and 533.09 eV are due to the OH^- and O^{2-} in H_2O molecules, respectively. All observed values of peak positions closely matched to values reported in literature, confirming the formation of phase-pure NiO [19].

3.7 Electrochemical measurements

The supercapacitive performance of electrodeposited NiO electrode was tested using cyclic C-V measurement. The capacitance (C) was calculated using following relation;

$$C = I / (dV/dt) \quad \ldots(3)$$

where I is the average current in ampere and dV/dt is the voltage scanning rate. The interfacial capacitance was calculated using the relation;

$$C_i = C/A \quad \ldots(4)$$

where 'A' is the area of active material dipped in the electrolyte. The SC (F g^{-1}) of NiO electrode was calculated using following relation;

$$SC = C/ W \quad \ldots(5)$$

where W is the mass of NiO film dipped in electrolyte.

3.7.1 Effect of scan rate

Due to a high-power demand in supercapacitors, one of the basic requirements for an electrode material in this field is the high or pulse-power characteristic [20, 21]. This unique property is a strong function of the electrochemical kinetics of redox transitions within the electro-active materials [22]. Thus, the high or pulse-power property of NiO electrode is examined using CV at different scan rates. The CV curves of NiO electrode in 0.5M Na_2SO_4 electrolyte at different scan rates within voltage range of −1.2 - +1.2 V are shown in Figure 4 (a). The area under curve increased slowly with the scan rate. This shows that the current is directly proportional to the scan rate, demonstrating an ideal capacitive behavior [23]. Figure 4(b) shows the variations of SC and Ci values with scan rate. From figure, it is seen that both values are decreased from 458 to 14 F g^{-1} and 0.0504 to 0.0015 F cm^{-2}, respectively. The maximum SC of 458 F g^{-1} was obtained at 5 mV/s. The decrease in SC was attributed to the presence of inner active sites that cannot sustain the redox transitions completely at higher scan rates. This is probably due to the diffusion effect of protons within the electrode. The decreasing trend of the SC suggests that parts of the surface of the electrode are inaccessible at high charging–discharging rates. Hence, the SC value obtained at the slowest scan rate is believed to be closest to that of full utilization of the electrode material [24]. Obtained results are better than the value previously reported by Patil et al (167 F g^{-1} in 2M KOH at scan rate of 5 mV/s) [25]

where synthesis of NiO was carried out using chemical bath method, suffering from the huge chemical wastage.

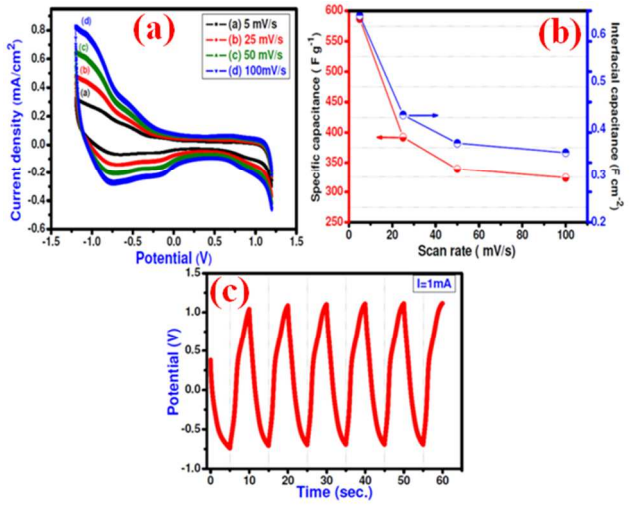

Figure 4: (a) CV, (b) variations of specific and interfacial capacitances at different scan rates, and (c) the charge–discharge measurements of NiO electrode in 0.5M $Na_2S_2O_3$ electrolyte.

3.7.2 Galvanometric charge–discharge studies

The charge–discharge behavior of NiO electrode was studied by galvanometric charge–discharge method at a constant current of 1 mA cm^{-2} between +0.4 and +1.1 V. Figure 4(c) shows the typical charge–discharge tests for NiO electrode. The discharge profile usually contains two parts; firstly, a resistive component arising from the sudden voltage drop representing the voltage changes due to the internal resistance and, secondly, a capacitive component related to the voltage change due to change in energy within the capacitor [26]. From Figure 4(c), the symmetric behavior of voltage–time curve is also seen. The Cs can also be measured by galvanostatic method by using relation;

$$Cs = I/(\Delta V/\Delta t) \times m \quad \ldots(6)$$

where Cs is specific capacitance, I is charge/discharge current, Δt is the discharge time, ΔV is potential drop during discharge, and m is the mass of active material within the electrode (m= 0.00011 g cm^{-2}). The maximum Cs of 454 F g^{-1} was confirmed at 1 mA cm^{-2} current density, which is in good agreement with that calculated from CV studies.

3.7.3Specific energy, power and energy efficiency

The electrochemical parameters such as specific energy (E), specific power (P) and coulomb efficiency (η%) are calculated using following equations;

$$E = (V \times I_d \times T_d)/W \quad \ldots(7)$$

$$P = (V \times I_d)/W \quad \ldots(8)$$

$$\eta\% = (T_d/T_c) \times 100 \quad \ldots(9)$$

where I_d , T_c, and T_d are the discharge current, charge time and discharge time, respectively. The W is the mass of NiO film electrode. The E value was 10.90 Wh kg^{-1}. The P and η% values of NiO electrode were 0.89 kW kg^{-1} and 98%, respectively.

3.7.4 Impedance analysis

Figure 5 (a) shows the electrochemical impedance spectroscopy (EIS) measurement of NiO at a fully charged state of 0.5 V/SCE. Measured impedance data of NiO was simulated using the equivalent circuit (inset of Figure 5 (a)). Very good agreement is observed between the measured and simulated data. The initial non-zero intercept at Z' at the beginning of the semicircle in the curve is due to the electrical resistance of electrolyte, which has a value of 0.5 Ω in 0.5M $Na_2S_2O_3$ electrolyte. The resistance projected by semi-circle was due to the active electrode material (Re). Therefore, the charge transfer resistance value of NiO was 4 Ω, implying presence of spherical aggregates, as the charge transfer resistance for spheres is generally low. Figure 5(b) shows a plot of phase angle *vs.* frequency; at phase angles of 46° and 51° about 61% and 60% of the powers correspond to heat production at the internal resistance with electrode loss factors of 1.02 and 0.20 were obtained in the higher and lower frequency region, respectively. This is in consistent with the effect of scan rate on SC, wherein the SC is higher for lower scan rate and lower for higher values. Therefore, lower scan rate is an appropriate region for good performance of NiO electrode.

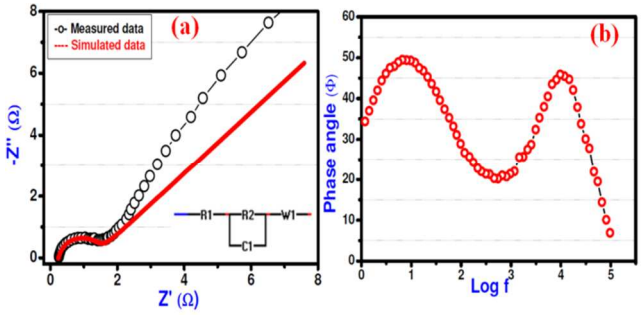

Figure 5: (a) Nyquist plot of NiO electrode at potential 0.5 V/SCE (inset shows the equivalent circuit) and (b) Plot of phase angle (Φ) *vs.* frequency (log f) of NiO electrode.

4. Conclusions

In this work, we have successfully synthesized NiO thin film electrodes using electrodeposition method and applied for electrochemical supercapacitor application. The XRD pattern confirmed amorphous nature of NiO. It was found from the FESEM image that NiO film surface was well-covered with irregular-sized spherical aggregates. The presence of characteristics bonds of NiO were confirmed by FTIR studies and further supported by XPS analysis. Contact angle measurement revealed the hydrophilic nature of NiO surface as surface water contact angle was smaller than 90°. The NiO electrode exhibited an interfacial capacitance of 0.64 F cm^{-2} and specific capacitance of 458 F g^{-1}. These results demonstrate that electrochemically deposited NiO thin film can be a good candidate as electrode material for electrochemical supercapacitor.

Acknowledgements
Authors (R.S. Mane and Mu. Naushad) extend their gratitude to the Visiting Professor (VP) Unit of King Saud University (KSU) and Deanship of Scientific Research, College of Science Research Center for supported. FJS would like to acknowledge Nanshan

District Key Lab for Biopolymers and Safety Evaluation (No.KC2014ZDZJ0001A).

References

1) H. Pang, Y. Ma, G. Li, J. Chen, J. Zhang, H. Zheng, W. Du, *Dalt. Trans.*, 2012, **41**, 13284.
2) H. B. Wu, H. Pang, X.W. Lou, *En. Env. Sci.*, 2013, **6**, 3619.
3) K.W. Nam, K. B. Kim, *J.Electrochem. Soc.*, 2002, **149,** A346.
4) H. Pang, B. Zhang, J. Du, J. Chen, S. Li, *RSc Adv*., 2012, **2** , 2257.
5) C. Lin, J.A. Ritter, B.N. Popov, *J. Electrochem. Soc.,*1998, **145**, 4097.
6) H.Y. Lee, J.B. Goodenough, *J. Solid State Chem.,*1999, **148**, 81.
7) K.W. Nam, K.B. Kim, *J.Electrochem. Soc.*, 2006, **153**, 81.
8) K.C. Liu, M.A. Anderson, *J. Electrochem. Soc.,*1996,**143**, 124.
9) A. Agrawal, H.R. Habibi, R.K. Agrawal, J.P. Cronin, D. Roberts, *Thin Solid Films*,1992, **221**, 239.
10) C. Natarajan, S. Ohkubo, G. Nagami, *Sol. State Ion.,* 1996, **86–88 (II)**, 949.
11) J.D. Desai, S.K. Min, K. D. Jung, O. S. Joo, *Appl. Surf. Sci.,*2006, **253**, 1781.
12) I. Zhitomirsky, *Mater. Lett.,*1998, **33**, 305.
13) B. E. Breyfogle, C. J. Hung, M.G. Shumsky, J. A. Switzer, *J. Electrochem. Soc.,*1996, **143**, 2741.
14) L. G. Or, I. Silberman, R. Chaim, *J. Electrochem. Soc.*, 1991, **138**, 1939.
15) B.O. Park, C.D. Lokhande, H.S. Park, K.D. Jung, O.S. Joo, *J. Power Sources*, 2004,**134**, 148.
16) B. O. Park, C.D. Lokhande, H. S. Park, K.-D. Jung, O. S. Joo, *J. Mater. Sci.,*2004, **39**, 4313.
17) Z.P. Feng, G.R. Li, J.H. Zhong, Z.L. Wang, Y.N. Ou, X. Tong, *Electrochem. Commun.,*2009, **11**, 706.
18) O. Bockman, T. Ostvold, G.A Voyiatzis, G.N. Papatheodorou, *Hydrometallurgy*, 2000, **55**, 93.
19) C.D.Wagner,W.M.Riggs, L.E.Devis and J.F.Moulder , Handbook of X-ray photoelectron spectroscopy, Physical Electronic Division, Perkin- Elmer Publisher, Eden Prairie, Minnesota, 1979, p-80.
20) I. Sapurina, A.Y. Osadchev, B.Z. Volchek, M. Trchova, A. Riede, J. Stejskal, *Synth. Met.,*2002, **129**, 29.
21) Z. Chen, L. Xu, W. Li, M. Waje, Y. Yan, *Nanotechnology*, 2006,**17**,5254.
22) C.C. Hu, T.W. Tsou, *Electrochem. Commun.*, 2002,**4**, 105.
23) K.C. Liu, M.A. Anderson, *J. Electrochem. Soc.,*1996,***143***, 124.
24) D.A. McKeown, P.L. Hagans, L.P.L. Carette, A.E. Russell, K. E. Swider, D.R. Rolison, *J. Phys. Chem. B*, 1999,**103**,4825.
25) U.M. Patil, R.R. Salunkhe, K.V. Gurav, C.D. Lokhande, *Appl. Surf. Sci.,*2008, **255**, 2603.
26) A. Bruke, *J. Power Sources*, 2000, **91**, 37.

Graphical Abstract